

Structured illumination microscopy (SIM) as an approach to functionally dissect periodic membrane structures in neuronal axons

Contact Ines Hahn ines.hahn@manchester.ac.uk and Andreas Prokop andreas.prokop@manchester.ac.uk

I. Hahn and A. Prokop

Faculty of Biology, Medicine and Health,
University of Manchester

S. E. D. Webb

Central Laser Facility, Science and Technology Facilities
Council, Research Complex at Harwell, Rutherford Appleton
Laboratory, Didcot, OX11 0QX, UK.

Introduction

Axons are slender cable-like projections of neurons that electrically wire the brain. Those delicate structures need to be maintained for a lifetime. Unsurprisingly, we gradually lose half of our axons during healthy aging and far more in neurodegenerative diseases (Adalbert and Coleman, 2012). We aim to understand the mechanisms of long-term axon maintenance, which will also be relevant for understanding axon pathology during aging and disease. We focus on the cytoskeleton and its immediate regulators, which have prominent hereditary links to neurodegenerative disorders (Prokop et al., 2013).

Axons contain parallel bundles of microtubules (MTs) that form their structural backbones and serve as life-sustaining transport routes. MT bundles are surrounded by regularly spaced actin rings termed periodic membrane skeleton (PMS) which were initially described in mammals. Their function was not known. We functionally dissected the structure and role of PMS by combining versatile *Drosophila* genetics with super-resolution microscopy.

SIM as a robust technique to image PMS in axons of *Drosophila* neuronal primary cultures

PMS is believed to represent a specific form of cortical F-actin: it was proposed to consist of short, adducin-capped actin filaments bundled into rings and cross-linked by spectrins that space them into regular ~ 180 -nm intervals (Xu et al., 2013; Lukinavičius et al., 2014; D'Este et al., 2015; He et al., 2016). However, this model is mainly based on super-resolution microscopy analyses, and very few actin regulators have been functionally assessed for their potential contributions to PMS architecture.

Here we take a new approach to analysing PMS. Previous analyses made use of stochastic optical reconstruction microscopy (STORM) or stimulated emission depletion (STED) microscopy. In contrast, we used structured illumination microscopy (SIM). As our cellular system, we used neurons of the fruit fly *Drosophila*, which we cultured for >6 days in vitro (DIV) and then fixed and stained with SiR-actin. These SIM-imaged axons revealed irregular dotted or elongated actin accumulations potentially demarcating synapses (arrows in Figure 1E), occasional longitudinal actin trails, as described also for mammalian neurons (boxed area 4 in Figure 1E; Ganguly et al., 2015), and abundant periodic actin patterns with a repeat length of 184 ± 2 nm, highly reminiscent of the PMS (Figure 1, A–E). Further validation clearly showed the PMS to be genuine. First, we found the same periodicity when using STED microscopy (Figure 1, C and D). Second, SIM imaging with anti-tubulin staining showed no periodicity (Figure 1F). Third, overlay images of the same preparation taken from three versus five angles showed a clear overlay (Figure 1, A and E).

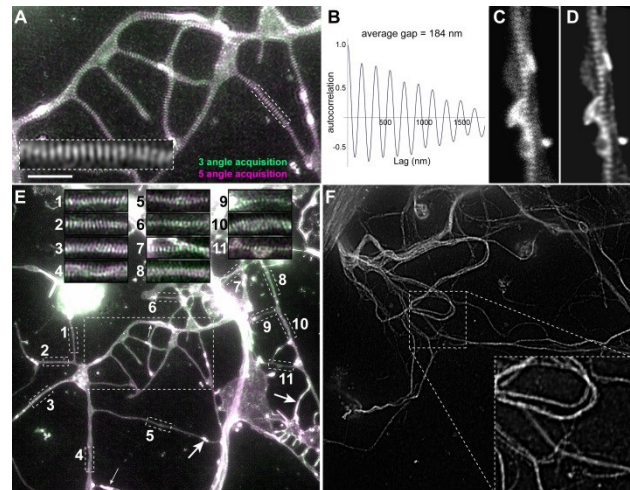


Figure 1: Superresolution images of *Drosophila* axons display PMS. (A) SIM image of SiR-actin-stained *Drosophila* primary neurons at 10 DIV; precise overlay of two independent rounds of image acquisition using three (green) vs. five (magenta) rotation angles; the framed area is shown fourfold magnified in the inset. (B) Autocorrelation analysis showing the regular periodicity of the actin staining with a lag of 184 nm. (C, D) Axon visualized via STED shown as raw (C) and deconvolved (D) images. (E) Full SIM image of SiR-actin-stained neurons at 10 DIV; the large boxed area is shown at larger scale in A; small boxed areas are shown as insets at the top, arrows mark dotted or elongated actin accumulations, and boxed area 4 might show an actin trail. (F) Full SIM image of neurons at 10 DIV stained with anti-tubulin; boxed area is shown as a 2.4-fold magnified inset at bottom right. Scale bars, 3 μ m (A, inset of F), 1.2 μ m (C, D, inset of A), 7.2 μ m (E, F), 2.1 μ m (insets of E).

Functional dissection of PMS

Compared to STED, SIM provides slightly lower resolution and does not permit measurements of actin content in PMS because it uses a demodulation algorithm with which the raw detected signal cannot be converted into photon counts. However, as an essential advantage for our studies, SIM allowed fast imaging and revealed PMS with high reliability in virtually all preparations (see overview in Figure 1E). This enabled us to reach sample numbers of several hundred to >1000 axon segments from different biological and technical repeats of each set of experiments. These conditions were ideal for systematic quantitative analyses, and we quantified the relative number of axon segments displaying PMS (termed PMS abundance) across axon populations of each experimental condition: The relative abundance of PMS was assessed on randomly chosen SIM images containing axons of SiR-actin-stained primary neuronal cultures, achieving sample numbers usually >300 . These were taken from four independent culture preparations obtained from at least two independent experimental repeats performed on different days. From each single culture preparation, at least 20 SIM images were obtained and, in each image, all neurite segments of >6 μ m length were counted. Generally, these neurite segments showed a consistent presence or absence of PMS all along. To avoid bias, image analyses

were performed blindly, that is, the genotype or treatment of specimens was masked.

Combining this efficient setup with versatile *Drosophila* genetics (Prokop et al., 2013), we were able to study the effect of the functional depletion of 11 actin regulators and three actin-targeting drugs on PMS abundance. We found a range of robust and highly reproducible effects on PMS, which provide functional support for the view that PMS represents cortical actin specializations: We found that PMS abundance depends on structural components like β -Spectrin and Adducin, actin nucleators like Formin or components of the Arp2/3 complex (ArpC2, Hem, SCAR), but not on actin elongators like profilin/Chic (see Figure 2 – F). This indicates that actin filaments in PMS are likely short, but high in number.

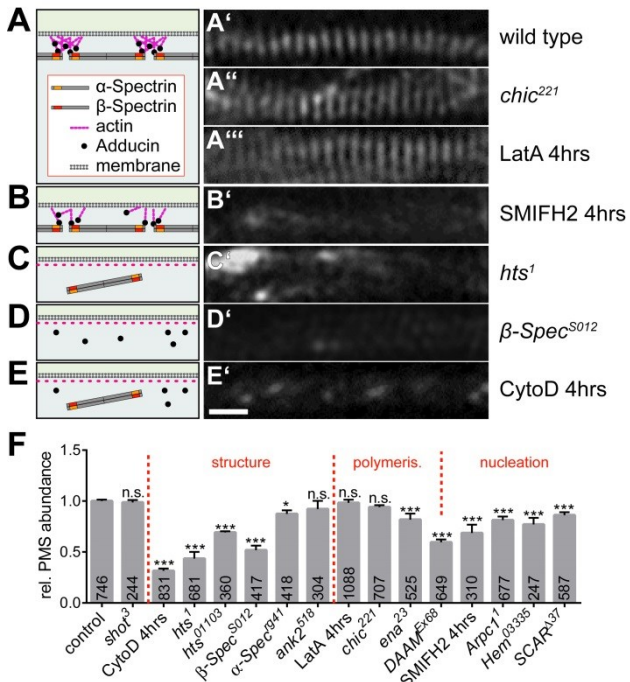


Figure 2: Functional dissection of PMS. (A–E) Representative SIM images of SiR-actin-labeled axons at 10 DIV genetically or pharmacologically manipulated as indicated on the right; scale bar, 550 nm (E', for all SIM images); schematics on the left provide an interpretation of the observed phenotype, based on the previously proposed cortical actin model (Xu et al., 2013). (F) Quantification of PMS abundance in axons of mature neurons at 10 DIV normalized to parallel control cultures; dotted lines separate different manipulations affecting regulators of structure, polymerization, or nucleation; p values were obtained via chi-squared analysis of raw data comparing axon segments with/without PMS (n.s., $p > 0.05$; * $p = 0.05$; ** $p = 0.01$; *** $p = 0.001$); numbers in bars represent sample numbers (i.e., analyzed axon segments); error bars represent SEM of independent experimental repeats.

Presence of cortical actin correlates with microtubule regulation

We then went on and applied the knowledge gained by our dissection of periodic membrane structures using SIM at CLF to explore the unknown yet potentially important roles of PMS or the cortical actin they represent (from now on referred to as PMS/cortical actin) in axons.

Upon actin removal, we observed gaps in microtubule bundles, reduced microtubule polymerization, and reduced axon numbers, suggesting a role of PMS in microtubule organization. These effects become strongly enhanced when carried out in neurons lacking the microtubule-stabilizing protein Short stop (Shot).

To analyze relations between PMS and MTs in a quantifiable manner, we used a further phenotype of *shot* mutant neurons, consisting of varicose regions of axons formed by disorganized

MTs that are not arranged into bundles but curl up and criss-cross each other (Figure 3A; Sánchez-Soriano et al., 2009; Voelzmann et al., 2016). Measurements of these areas are easy to perform and statistically robust across large neuron populations and we express them as the MT disorganization index (MDI; area of disorganized MTs relative to axon length). We found a close correlation between MDI and PMS abundance when we analysed neurons in which the *shot³* mutant allele was combined with various mutations of actin regulators. For example, combining *shot* mutants with loss of actin nucleators like *SCAR^{Δ37}* neurons showed a highly significant reduction in MDI at both 8 HIV and 3 DIV, correlating well with the significantly reduced PMS abundance observed in *SCAR^{Δ37}* mutant neurons (Figures 2F, 3G and H). In contrast, *shot³ chic²²¹* double-mutant neurons showed no significant MDI reduction (Figure 3, B, G, and H), in agreement with the fact that the *chic²²¹* mutation does not affect PMS abundance (Figures 2, A and F, and 4D). In total we analyzed the MDI in 16 different conditions in which drugs or actin-regulator mutations were combined with *shot³* mutant background (Figure 8). We then plotted these MDI data (Figure 3) against the respective PMS abundance data obtained for wild-type neurons at 8 HIV and 10 DIV (Figure 2) and found a highly significant correlation between the presence/absence of PMS and high/low values for MDI (Spearman $r = 0.782$, $p = 0.0009$). These correlations suggest that MT-regulating capacity is a function of the amount of PMS present in axons.

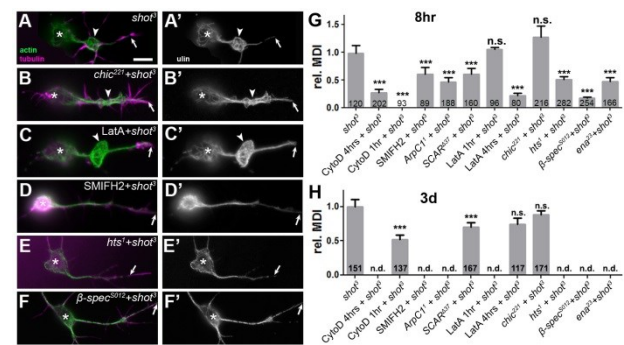


Figure 3: F-actin manipulations in *shot*-mutant neurons. (A–F') The *shot*-mutant primary neurons at 8 HIV stained for tubulin (green) and actin (magenta) combined with different actin manipulations as indicated (asterisks, cell bodies; arrows, axon tips; arrowheads, areas of MT disorganization). (G, H) Quantification of MDI for neurons at 8 HIV (H) and 3 DIV (I); numbers in bars refer to neurons analyzed; all data normalized to *shot*; for detailed data. p values were calculated using the Mann–Whitney rank sum test (n.s., $p > 0.05$, *** $p < 0.001$). Scale bar, 10 μ m (A–G').

Conclusions

Our combined approach using efficient super-resolution SIM imaging with versatile *Drosophila* genetics enabled us to functionally dissect PMS in axons. The advantage of SIM imaging, which provides slightly less resolution than STORM or STED is that it is fast and reliable and therefore ideally suited for quantitative analysis with very high sample numbers. This enabled us to apply a wide range of genetic and pharmacological manipulations and classify their affects using PMS abundance as readout. We could then apply our knowledge by showing a first functional relevance of PMS for MT bundles, MT dynamics, and even axon maintenance.

The work was published in: Qu, Y*, Hahn, I*, Webb, S., Prokop, A. (2017). Periodic actin structures in neuronal axons are required to maintain microtubules. *Mol Biol Cell* doi:10.1091/mbc.E16-10-0727/ p296-308

Acknowledgements

We thank Stephen Webb, Sarah Needham and Christopher Tynan for their support. This work was funded by the Biotechnology and Biological Sciences Research Council

(BBSRC) (BB/L000717/1, BB/ M007553/1) to A.P., as well as support by parents and Manchester's Faculty of Life Sciences (now Faculty of Biology, Medicine and Health) to Y.Q. Structured illumination and STED microscopes at the Research Complex at Harwell were funded by the Medical Research Council (MR/K015591/1) and the BBSRC (BB/L014327/1), and imaging time was made possible through three successive grants by the Science and Technology Facilities Council to A.P.

References

1. Adalbert R, Coleman MP (2012). Axon pathology in age-related neurodegenerative disorders. *Neuropathol Appl Neurobiol* 39, 90–108.
2. D'Este E, Kamin D, Göttfert F, El-Hady A, Hell SW (2015). STED nanoscopy reveals the ubiquity of subcortical cytoskeleton periodicity in living neurons. *Cell Rep* 10, 1246–1251.
3. Ganguly A, Tang Y, Wang L, Ladtschik K, Loi J, Dargent B, Leterrier C, Roy S (2015). A dynamic formin-dependent deep F-actin network in axons. *J Cell Biol* 210, 401–417.
4. He J, Zhou R, Wu Z, Carrasco M, Kurshan P, Farley J, Simon D, Wang G, Han B, Hao J, et al. (2016). Prevalent presence of periodic actin-spectrin-based membrane skeleton in a broad range of neuronal cell types and animal species. *Proc Natl Acad Sci USA* 113, 6029–6034.
5. Lukinavicius G, Reymond L, D'Este E, Masharina A, Göttfert F, Ta H, Güther A, Fournier M, Rizzo S, Waldmann H, et al. (2014). Fluorogenic probes for live-cell imaging of the cytoskeleton. *Nat Methods* 11, 731–733.
6. Prokop A, Beaven R, Qu Y, Sánchez-Soriano N (2013). Using fly genetics to dissect the cytoskeletal machinery of neurons during axonal growth and maintenance. *J Cell Sci* 126, 2331–2341.
7. Sánchez-Soriano N, Travis M, Dajas-Bailador F, Goncalves-Pimentel C, Whitmarsh AJ, Prokop A (2009). Mouse ACF7 and Drosophila Short stop modulate filopodia formation and microtubule organization during neuronal growth. *J Cell Sci* 122, 2534–2542.
8. Voelzmann A, Hahn I, Pearce S, Sánchez-Soriano NP, Prokop A (2016). A conceptual view at microtubule plus end dynamics in neuronal axons. *Brain Res Bull* 126, 226–237.
9. Xu K, Zhong G, Zhuang X (2013). Actin, Spectrin, and associated proteins form a periodic cytoskeletal structure in axons. *Science* 339, 452–456